Pak. J. Agri. Sci., Vol. 56(4), 993-1001; 2019
ISSN (Print) 0552-9034, ISSN (Online) 2076-0906
DOI:10.21162/PAKJAS/19.8351
http://www.pakjas.com.pk

SOLAR PHOTOCATALYTIC TREATMENT OF TEXTILE EFFLUENT FOR ITS POTENTIAL REUSE IN IRRIGATION

Ambreen Rafiq[1,*], Ijaz Ahmad Bhatti[1], Asif Ali Tahir[2], Munir Ashraf[3], Haq Nawaz Bhatti[1] and Muhammad Anjum Zia[4]

[1]Department of Chemistry, University of Agriculture, Faisalabad, Pakistan; [2]Energy and Sustainability Institute, University of Exeter, United Kingdom; [3]National Textile University, Manawala, Pakistan; [4]Department of Biochemistry, University of Agriculture, Faisalabad, Pakistan.
[*]Corresponding author's e-mail: ambreenashar2013@gmail.com

Since textile industry is the greatest consumer of water, it generates large quantities of effluents. The advanced methods of water treatment present a great potential in terms of wastewater reuse for irrigation. Heterogeneous photocatalysis is a promising technique to mortify the dye residues from textile effluent. In this study, Fe^{3+} doped ZnO has been synthesized through microwave assisted sol-gel method. The crystallinity and elemental composition of fabricated material was determined by X-ray diffraction (XRD). Two-dimensional disc shaped morphology of photocatalyst has been examined by scanning electron microscopy (SEM) of Fe^{+3} doped ZnO. Diffused reflectance spectroscopy confirmed its high photocatalytic activity in solar range on reduction of band gap from 3.2 to 2.8 eV after doping. The characterized Fe^{+3} doped ZnO samples have been used to degrade RB5 dye on irradiating with artificial sunlight (D65). The reaction parameters i.e. initial dye and oxidant concentration, pH and irradiation time have been optimized by Response surface methodology (RSM). The extant of dye degradation has been evaluated by UV/vis and FTIR spectroscopy. The maximum degradation up to 98.32 % in 3 h was achieved on using ZnO doped with 5 mM of Fe^{+3} under optimized conditions. The phytotoxicity of treated and untreated effluent on length of root and shoot of spinach in addition to yield was measured. The remarkable increase in vegetative growth of plants was observed on using treated textile effluent.

Keywords: Textile effluent, solar photocatalysis, response surface methodology, phytotoxicity.

INTRODUCTION

In water stressed countries it is a common practice to irrigate plants with grey water being released from residential and industrial sources instead of discharge into water body (Faryal *et al.*, 2007). In textile industry up to 60 to 70% of dyes used contain azo group (-N=N). It has been reported that 15–50% of the applied azo dyes do not bind to the fabric. The concentration of the azo dyes in textile wastewaters vary from 10 to 250 mg L^{-1} (O'Neill *et al.*, 1999). The presence of azo dyes in surface water cause aesthetic troubles as well as obstruct penetration of light and decrease concentration of dissolved oxygen in water (Li *et al.*, 2012; Zhang *et al.*, 2012). Moreover, azo dyes and their degradation intermediates are also mutagenic and carcinogenic for living organisms (Weisburger, 2002).

As a whole it was estimated that 26% of the total vegetable production was produced with untreated wastewater in Pakistan. A diverse range of vegetables are grown with wastewater in Pakistan among which spinach and cauliflower are most commonly cultivated in peri-urban areas (Ensink *et al.*, 2004). The dyes stabilize in colloidal portion of soil during a period of a few weeks and retained in for long time (Imran *et al.*, 2015). These dye contaminants negatively affect seed germination rates and vegetative growth of plants (Vafaei *et al.*, 2012). A number of researchers have investigated the negative effect of azo dyes on germination and plant growth through processes occurring in soil to discover the mechanistic basis of dye contamination (Mahmood *et al.*, 2017; Shafqat *et al.*, 2017).

Since textile effluents are blend of diverse toxic components, the role of each component to varies with dispersion and dilution in aqueous medium and their discharge in environment. The effects on inhibition of seed germination in addition to vegetative growth are important for investigation in the area of research on phytotoxicity. The ratio tests of root and shoot have been used as reliable, simple and reproducible process for evaluation of phytotoxicity caused by toxic moieties present in textile effluent (Reemtsma, 2001).

The heterogeneous photocatalysis employing semiconductor metal oxides has been proved to have remarkable advantages such as mineralization of broad spectrum of organic pollutants even at ambient temperature and pressure (Adeleye *et al.*, 2016). The photocatalysts that enhance the generation of free radicals on absorbing radiation in visible region are the most desirable (Amin *et al.*, 2015). Semiconductor nano metal oxides like ZnO, are of great importance as efficient *in situ* generation of hydroxyl free radical on irradiation at neutral

pH and can be utilized for the degradation of organic pollutants (Kołodziejczak-Radzimska and Jesionowski, 2014). The photocatalytic activity (PCA) greatly depends on morphology, surface area and bandgap (Ashar *et al.*, 2016). Doping of pure ZnO with suitable cations increase the crystal defects, decrease band gap and enhance PCA (Sun *et al.*, 2016).

The present study involves the synthesis of 2D, Fe^{3+}doped ZnO by microwave assisted sol-gel method. The as-synthesized photocatalyst was used to degrade CI Reactive Black 5 (RB5) bisazo dye in artificial solar photocatalytic reactor. The dopant Fe^{3+} aided the redox reaction at the surface of photocatalyst enhancing the harvesting of the solar radiation. Then real textile effluent was treated by Fe^{3+}dopedZnO nano photocatalyst and effect of treated and untreated effluent on vegetative growth of spinach as a pot plant was determined.

MATERIALS AND METHODS

Analytical grade zinc sulphate heptahydrate $Zn(SO_4)_2.7H_2O$ (99.9%), ferric nitrate nonahydrate $Fe(NO_3)_3.9\ H_2O$ (99.95%), sodium hydroxide (NaOH) (99%) and hydrogen peroxide H_2O_2 (36%) were purchased from Sigma-Aldrich. RB5 dye was purchased from Dow Chemicals. D65 lights of (72 watts) were used as a source of simulated solar radiation. The textile effluent sample collected from local industry and treated effluents were stored at 4°C in plastic cans. The spinach plants (*Spinacia oleracea*) of same average height (5 cm) were selected from nursery, grown in triplets in pots of same dimensions.

***Method employed for synthesis of undoped and Fe^{+3} doped ZnO*:** To synthesize powdered doped ZnO**,** 0.25 M $Zn(SO_4)_2.7H_2O$ and 0.5M NaOH solutions were prepared in deionized water as precursor solutions and were mixed during stirring. Then 1-6 mM of Fe^{+3} solution was added to 200 ml of solution and the resultant suspension was subjected to microwave irradiation of 90 watts for 10 min. The light yellow colored residue obtained was dried at 80°C in a vacuum oven for 5 h and ground to fine powder. For undoped ZnO, same method was followed without adding Fe^{3+} solution, white residue was obtained after drying.

***Characterization of fabricated material*:** To determine crystalline properties elemental composition of nanoZnOJeol JDX- 3532 diffractometer (Japan) was used. Microscopy has been done by Quanta 250. FEG (USA),while diffused reflectance spectrometry (DRS) and UV/vis spectrophotometic determination was executed by Perkin Elmer Lambda 1050(USA).The effect of photocatalytic treatment on composition of products of dye were studied by Fourier Transform Infrared Spectroscopy (FTIR) (Bruker IFS 125HR Japan).

***Photocatalytic degradation of dye*:** Photocatalysis has been carried out in borosilicate glass containers of 20x20x4 cm^3 containing 100 ml of RB5 dye solution for each experiment. To optimize the effects of pH, dye concentration, catalyst load and supporting oxidant on photocatalytic degradation, Response Surface Methodology (RSM) has been used for investigating the interactive effect of reaction parameters keeping sunlight irradiation time constant as180 min. The runs (30) suggested by Design Expert 7 were performed to find out the percentage degradation of RB5 as a response. The level of pH were examined from 5 to 9, H_2O_2 concentration 10 to 50 mM,catalyst load 10 to 50 mg and intial concentration of dye was 10 to 50 ppm. Response in photocatalytic experiments was percent degradation of dye RB5 which was calculated using following equation.

$$\text{Degradation (\%)} = \frac{A_o - A_f}{A_0} \times 100$$

Where, A_o: absorbance of dye solution before treatment and A_f: absorbance of dye solution after treatment.

The treatment of synthetic textile effluent containing only bis azo dye was executed under optimized conditions to specifically address the effect of dye on vegetative growth of plants. The initial concentration of dye in synthetic effluent used was 150 ppm and pH determined was 8.5. The treated effluent contained less than 1ppm of RB5 while pH determined was 7.1.

***Irrigation of pot plants using textile effluent*:** The treatment of synthetic textile effluent containing only bis azo dye was executed under optimized conditions to specifically address the effect of dye on vegetative growth of plants. The initial concentration of dye in synthetic effluent used was 150 ppm and pH determined was 8.5. The treated effluent contained less than 1ppm of RB5 while pH determined was 7.1.

The treated and untreated synthetic textile effluent were used for irrigation of pot spinach plants divided in 3 groups (A, B and C) each consisting of 3 plants. The group A was irrigated with untreated textile effluent, while group B was treated with treated textile effluent. In addition tap water was used as a control for group C. The volume of water used for irrigation of A, B and C group was 200 ml daily. The experiment was performed in triplicate, root and shoot length was measured after 15, 30 and 45 days using measuring scale while number of leaves were measured by counting. The results are reported as relative percent root and shoot elongation and percent yield using the formulas given as under:

Relative root/shoot growth (%) using untreated effluent = Mean length in untreated effluent/Mean length in control x100

Relative root/shoot growth (%) using treated effluent = Mean length in treated effluent/Mean length in control x100

Relative % yield using untreated effluent = Mean number of leaves in untreated effluent/Mean number of leaves in control x100

Relative % yield using treated effluent = Mean number of leaves in treated effluent/Mean number of leaves in control x100

RESULTS AND DISCUSSION

The present study included synthesis of Fe^{3+}dopedZnO using MWSG method, while the dopant concentration range investigated was 0-6 mM of Fe^{3+}. The results of characterization and determination of PCA have been described as under.

***Structural properties of Fe^{3+}doped ZnO*:** According to the diffractogram obtained from XRD, all of the main peaks appearing at 2θ = 31.68°, 34.31°, 36.31° for undoped sample belonged to the ZnO wurtzite phase. The highest peak appeared at 36.31° (2θ) which gave crystallite size 26.60 nm by Scherrer's formula finding full width half maximum (FWHM) as 0.354 using XpertHighscore software. The constants of hexagonal lattice for ZnOnano structures obtained were as given in JCPDS (card no. 36-1451) i.e. a=3.35100Å c=5.22600Å. On doping ZnO with Fe^{3+} the lattice parameters should be close to JCPDS values of pure ZnO (Rekha *et al.*, 2010). Diffractograms of as-synthesized Fe^{3+}doped ZnO powders with varying dopant concentrations are given in (Figure 1).

It can be seen in diffractograms that on doping ZnO with Fe^{3+} in the concentration 1-5mM, no extra peak appeared corresponding to iron oxide on increasing the dopant concentration upto 5 mM. On further increasing the concentration of Fe^{3+} to 6 mM, small peaks of impurity appeared. Previous researchers have also reported that appearance of small peaks on increasing dopant percentage in ZnO lattice (Karmakar *et al.*, 2007). Doping of ZnO with Fe^{3+} caused a slight change in its crystal structure as a result of defect creation. The peak position, FWHM values and lattice constants have been given in Table 1.

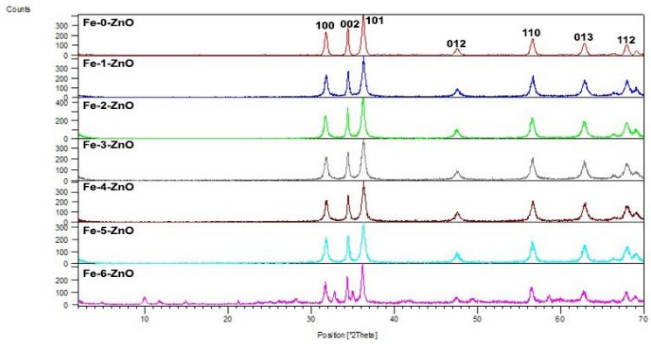

Figure 1. Diffractograms of undoped and Fe^{3+}doped ZnO samples containing of 1-6 mM of Fe^{+3}.

As it is clear from data, the increased values of FWHM, revealed the decrease in crystallite size sequentially on increasing the concentration of dopant. On inducting 5 mM of Fe^{3+} the highest peak shifted from 36.31° to 36.25° (2θ) position of lattice with FWHM 0.433 and crystallite size 19.30 nm. That was the minimum crystallite size obtained among all the Fe^{3+} doped samples of ZnO. The results obtained are in agreement with previous examinations reported according to which variation in lattice parameters was observed on Fe^{3+} doping (Lavand and Malghe, 2016). Due to the minimum crystallite size, increased surface area and maximum crystal defects, Fe^{3+}-5-ZnO was selected for further characterization, since it was expected to exhibit highest PCA.

***Morphological properties of Fe^{3+}-5-ZnO*:** Micrographs of SEM declared the 2D morphology of Fe^{3+}-5-ZnO due to the reaction between the precursors selected. The mono-modal discs of almost same size can be seen in SEM (Fig. 2a). The discoid hexagons of the fabricated material, agglomerated due to high surface charge, as expected due to greater extent of exposed surface polar area. The discs formed are of very less

Table1. Lattice parameters of Fe^{+3} doped ZnO samples.

S. No.	Sample doping	Peak position (2θ)	FWHM	Crystallite size (nm)	Crystal constants
1	Fe^{3+}-0-ZnO	36.319	0.319	28.32	a= 3.25330 Å c= 5.20730 Å
2	Fe^{3+}-1-ZnO	36.314	0.354	26.60	a= 3.25330 Å c= 5.20730 Å
3	Fe^{3+}-2-ZnO	36.310	0.362	23.05	a= 3.24950 Å c= 5.20710 Å
4	Fe^{3+}-3-ZnO	36.291	0.383	21.34	a= 3.24940 Å c= 5.20380 Å
5	Fe^{3+}-4-ZnO	36.276	0.392	20.80	a= 3.24931 Å c= 5.20571 Å
6	Fe^{3+}-5-ZnO	36.256	0.433	19.30	a= 3.24370 Å c= 5.19910 Å
7	Fe^{3+}-6-ZnO	36.247	0.295	28.31	a= 3.24330 Å c= 5.20704 Å

thickness with rough surface and the average dimensions of discs were 94x 120 nm as shown in Figure 2b.

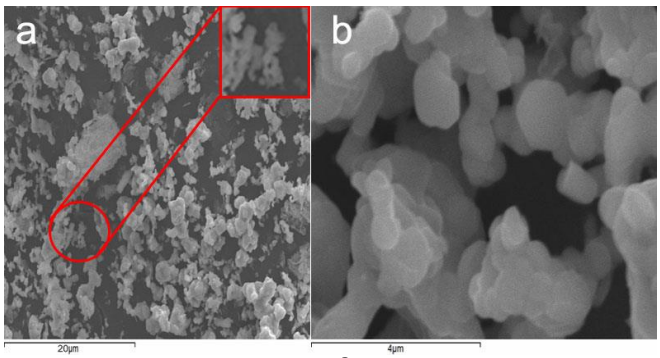

Figure 2. Images of SEMa) Fe^{3+}-5- ZnOnano discs at 5KX b) agglomerated Fe^{+3}-5- ZnOnano discs at 25 KX.

***Optical properties of Fe^{3+}-5-ZnO*:** Determination of diffused reflectance (DRS) of Fe^{3+} doped ZnO samples exhibited that with the increase in concentration of dopant from 1 to 5 mM the extent of absorbance of visible portion of solar spectrum increases (Fig. 3). It is quite obvious that all of Fe^{+3} doped ZnO samples showed lesser % reflectance throughout in the solar spectrum.

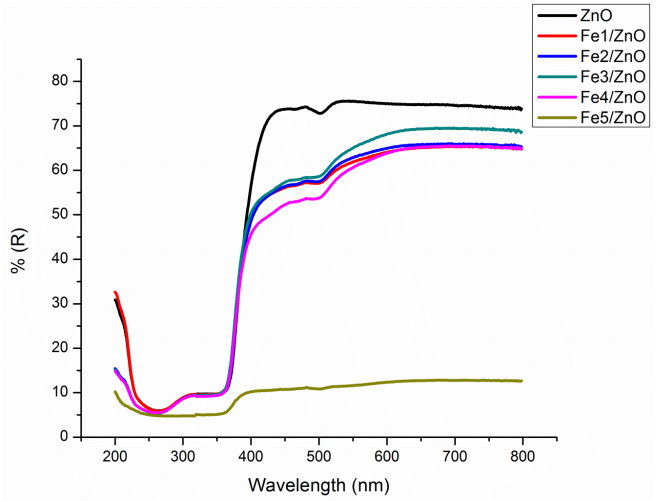

Figure 3. Comparison of diffused reflectance spectra of undoped and Fe^{3+}doped ZnO.

The ZnO sample having 5 mM of Fe^{3+} has shown the magnificent decrease in reflectance and inversely 90% absorbance in visible portion of solar radiation. The shift in absorption edge can be correlated to electronic transition from valence band to dopant energy level bellow conduction band of ZnO. Thereby, it can be concluded that appearance of dopant energy level decreases the bandgap energy (Wu *et al.*, 2014). Furthermore, analyses of the optical bandgaps of synthesized Fe^{3+} doped ZnO samples by Kubelka-Munk plot were 3.15, 3.08, 3.04, 3.09, 2.96, 2.70 and 3.06 eV for 0-6 mM of Fe^{3+} induced in the crystal of ZnO (Fig. 4). Conclusions based on previous results for Fe^{3+} doping revealed that visible light harvesting is strongly influenced by the concentration of Fe^{3+} dopant. The enhanced rate of photocatalytic reaction can be attributed to reduced bandgap energy and high rate of $OH^{\bullet}$ generation (Karmakar *et al.*, 2007).

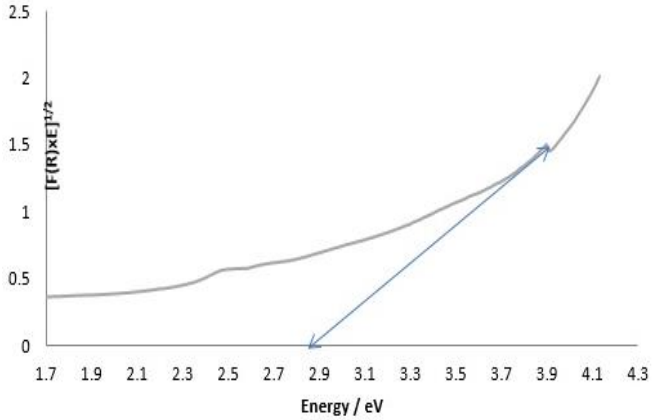

Figure 4. Bandgap energy of Fe^{3+}-5-ZnO sample.

***Photocatalytic properties of undoped and Fe^{+3} doped ZnO*:** For determination of comparative PCA of undoped and Fe^{3+} doped ZnO powdered samples, the photocatalytic degradation reaction of RB5 bisazo anionic dye was carried out. The optimized reaction parameters were employed for the photocatalytic degradation of RB5, investigated during solar irradiation for 180 min.

***Optimization of reaction parameters using undoped ZnO*:** The 30 experimental runs provided by Design expert 7, software were performed using undoped ZnO sample for optimization of reaction parameters. The response was inserted as % degradation based on the decolorization of RB5 dye solution measured as absorbance shown by RB5 at 600 nm.

After inducing the response of the experimental runs in the software it provided with ANOVA (Table 2). The ANOVA provided, sum of squares, mean square and F values for four independent variables (A, B, C, D) interactive variables (AB, AC, AD, BC, BD and CD) and square of individual reaction parameters. According to ANOVA, the model proposed was significant and lack of fit was significant.

The optimized levels of individual variable parameters obtained through RSM were pH= 7, H_2O_2 concentration of 30 mM, catalyst load 30 mg/100 ml and initial dye concentration =30 ppm. Highest rate of degradation was achieved for RB5 at pH 7 because surface of ZnO at pH lesser than point of zero charge (Pzc) attain positive charge. To adsorb anionic RB5 dye for adsorption prior to photocatalysis the positively charged surface acts as Lewis acid and allows dye molecule

Table 2. ANOVA for optimization of photocatalytic reaction variables for undoped ZnO.

Source	Sum of squares	Df	Mean Square	F Value	p-value Prob > F	
Model	9486.36	14	677.60	8.96	< 0.0001	significant
A-pH	4.97	1	4.97	0.066	0.8012	
B-Oxidant (H_2O_2)	10.67	1	10.67	0.14	0.7124	
C-Initial Conc. of Dye	263.77	1	263.77	3.49	0.0815	
D-Catalyst Loading	1635.83	1	1635.83	21.63	0.0003	
AB12.08		1	12.08	0.16	0.6951	
AC103.53		1	103.53	1.37	0.2602	
AD2.28		1	2.28	0.030	0.8645	
BC0.72		1	0.72	9.555	0.9234	
BD10.08		1	10.08	0.13	0.7201	
CD79.12		1	79.12	1.05	0.3226	
$A^2$4549.66		1	4549.66	60.17	< 0.0001	
$B^2$397.21		1	397.21	5.25	0.0368	
$C^2$409.74		1	409.74	5.42	0.0343	
$D^2$3188.41		1	3188.41	42.17	< 0.0001	
Residual	1134.20	15	75.61			
Lack of Fit	994.99	10	99.50	3.57	0.0862	non-significant
Pure Error	139.21	5	27.84			
Core Total	10620.55	29				

to behave as Lewis base, forming an intermediate complex. As indicated by the results of experiments more hydroxyl radicals ($OH^{\bullet}$) are generated with the increasing pH, which increases the PCA regarding the photodegradation of RB5. Since pzc of ZnO is 9.5, pH 7 as an optimum pH for a redox reaction of anionic dye is justified.

Rate of photocatalytic degradation of RB5 was accelerated with the addition of H_2O_2 as it acts as an inhibitor of recombination and aided in the *in situ* generation of oxidizing agent $OH^{\bullet}$. Self-decomposition of H_2O_2 took place on irradiation and due to reduction of H_2O_2 on trapping electron from conduction band (CB) results in increased concentration of $OH^{\bullet}$ in reaction mixture. Highest degradation of RB5 required 30 mMH_2O_2 concentrations while its dosage beyond the optimum level results in retarded rate of degradation.

Initial concentration of pollutant dye also has a crucial role in its degradation on the surface of heterogeneous photocatalyst. Following the Langmuir's theory of adsorption, rate of degradation of dye was declined gradually, when the concentration of dye exceeded 30 ppm. All of these parameters were indicated by the software to have interactions. Keeping two parameters constant, the other two were varied and effects of interactions have been displayed in 3D surface plots given as under:

***Interactive effects of reaction parameters*:** In the first set of experiments, keeping initial concentration of RB5 dye (30 ppm) and catalyst load (30 mg) as constant, when pH and H_2O_2 concentration were varied maximum degradation was 80.65% on attaining pH 7 and H_2O_2 concentration 30 mM (Fig. 5a).

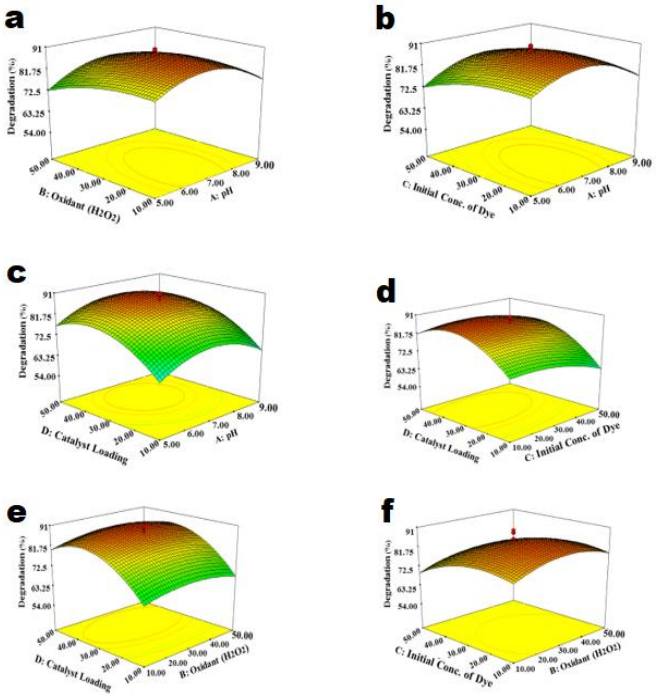

Figure 5. The interactive effect of a) oxidant H_2O_2 concentration and pH b) Initial concentration of dye and pH c) Catalyst loading and pH d) initial concentration of dye and catalyst loading e) Catalyst loading and H_2O_2 concentration f) Oxidant and initial dye concentration for powder undoped ZnO samples.

When initial concentration of dye and pH were varied and catalyst load and H_2O_2 concentration were kept constant degradation increased to 80.67% (Fig. 5b). When catalyst loading and pH were varied simultaneously and initial concentration of dye and H_2O_2 concentration were kept constant maximum dye degradation attained was 81.34% (Fig. 5c). On taking H_2O_2 concentration and pH constant and varying catalyst load along with initial concentration of dye, maximum degradation achieved was 80.41% (Fig. 5d). On the other hand, varying catalyst load and H_2O_2 concentration at initial concentration of dye and pH constant, maximum degradation achieved was 80.65% when initial dye concentration was 30 mM and pH was 7 (Fig. 5e). Moreover, when initial concentration of dye and H_2O_2 concentration were varied keeping the other two factors constant the degradation achieved was 81.25% (Fig.5f) Taking the average maximum degradation achieved was 80.82% on using undoped ZnO as a photocatalyst.

***Photodegradation of RB5 by Fe^{3+}doped ZnO samples*:** Under the optimized conditions, the ratio of concentration of RB5 dye after photocatalytic treatment to the initial concentration (C/C_0) have been used to determine PCA of Fe^{3+} doped ZnO samples in comparison of undoped ZnO. It is obvious from the decreasing values of C/C_0 that all of the Fe^{3+} doped ZnO samples have exhibited higher PCA than intrinsic ZnO except Fe^{+3}-6-ZnO. This fact can be attributed to multiple factors, which has been explained in previous sections.

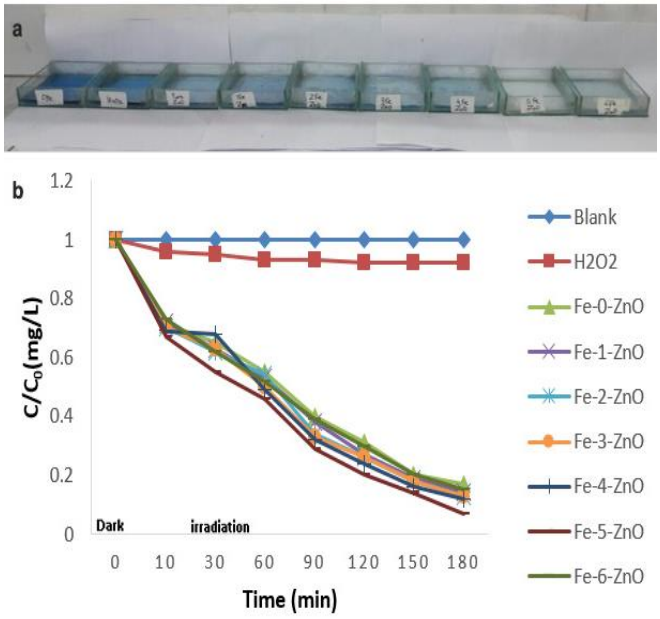

Figure 6. a) Comparison of extent of decolorization of RB5 by undoped and Fe^{3+} doped ZnO b) Comparison of C/C_0 for determination of PCA of undoped and Fe^{3+}doped ZnO samples with respect to time.

The maximum PCA was noticed for Fe^{+3}-5-ZnO, since it has shown minimum value for C/C_0. The results obtained after photocatalytic treatment of RB5 dye has been displayed (Fig. 6 a,b). It can be observed that maximum decolorization has been obtained on using Fe^{+3}-5-ZnO. The values of C/C_0 obtained from absorbance of 30 ppm dye solution measured on UV/vis spectrophotometer at 600 nm before and after the photocatalytic reaction has been plotted with respect to time (min).

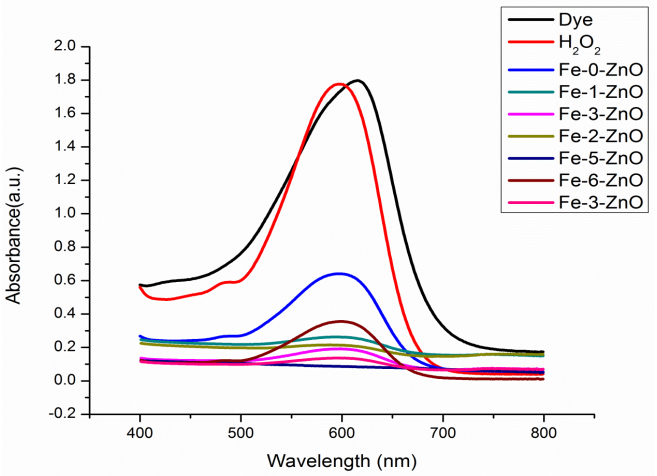

Figure 7. Comparison of extent of decolorization of RB5 dye after photocatalytic treatment using undoped and Fe^{3+}doped ZnO samples.

***The evaluation of extent of decolorizaton of RB5*:** The evaluation of extent of decolorizaton has been determined through UV/vis spectra of blank as 30 ppm dye solution, dye solution containing merely H_2O_2 as an oxidant and dye solutions after photocatalytic treatment using Fe^{3+} doped ZnO photocatalysts (Fig. 7). The extent of decolorization was enhanced with increasing dopant concentration from 1-5 mM. The maximum decolorization was shown by Fe^{3+}-5- ZnO in 180 min.

The extent of degradation of RB5 in treated textile effluents was further determined by FTIR of the treated and untreated synthetic effluents. Spectrum of FTIR of untreated dye has shown a strong band at 3355.92 cm^{-1}due to N–H stretching and small peaks at 1114.33 cm^{-1} due to C–N stretching. The peak at 1456.33 appeared due to N=N stretching and peak at 1654.27 cm^{-1} appeared due to –NH bending. The treated textile effluent has shown prominent decrease in all the peaks indicating cleavage of azo groups. Similarly a small band near 750 cm^{-1} is the peak of benzene ring appeared as a product of photocatalytic reaction. A strong band at 3355.92 cm^{-1} have almost vanished in treated dye. No peak corresponding to aryl amines was observed, whereas a small peak at 1541.45 cm^{-1} has appeared corresponding to aromatic rings. The spectrum of treated effluent indicated conclusively that RB5 has been degraded to simpler aromatic hydrocarbons. Absence of peak

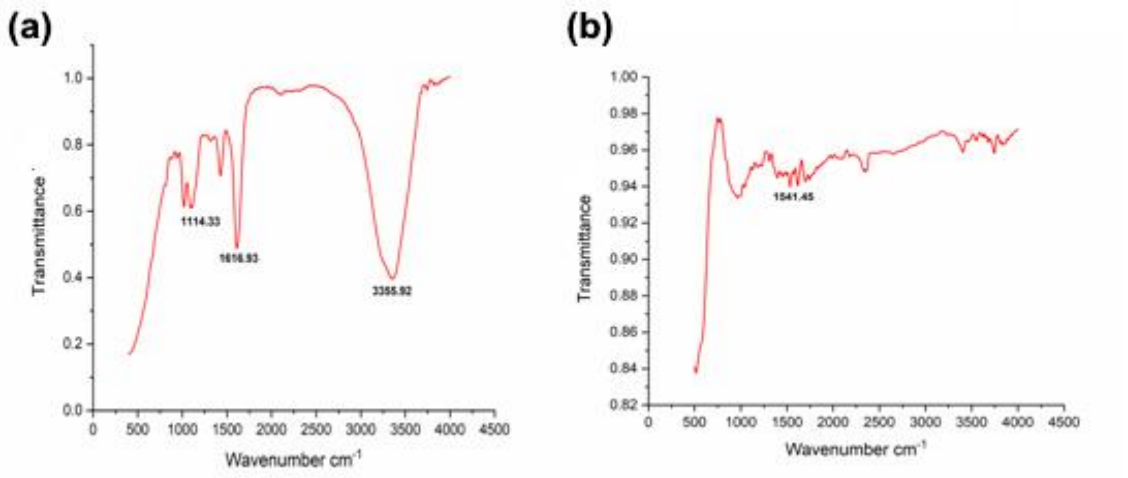

Figure 8. FTIR of a) untreated textile effluent containing RB5 dye b) treated textile effluent.

at 3000-3100 cm^{-1} indicated that ethylene and its derivatives were not produced after photocatalysis (Fig. 8). The spectral setup observed was found similar to that reported in other photodegradation reports (Gahlout *et al.*, 2013; Neoh *et al.*, 2015).

***Effect of untreated and treated textile effluent on irrigation of spinach plant*:** Effect of irrigation water on spinach plant was determined by measuring shoot length, root length and yield as number of leaves. The observations were recorded after 4 weeks and average of treatments was plotted. The data obtained has been plotted as relative root and shoot growth % and yield % using untreated and treated textile effluent for irrigation of spinach plant**:**

The data presented in graph delineated the effect of RB5 dye on vegetative growth of plants. It is clear from results that shoot length was retarded when irrigated with untreated textile effluent containing high concentration of RB5. It was observed that % relative shoot length increased substantially on applying treated effluent for irrigation (Fig. 9). The relative % root length was also examined to be affected by irrigation with treated and untreated textile effluent. On removal of dye from effluent, an increase in the growth of root was also observed but shoot length was found to be affected to a greater extent. The relative % yield of a plant corresponding to the number of leaves obtained was 100% when irrigated with treated textile effluent. However, the yield obtained on irrigating the plants of same initial height with untreated textile effluent was much lesser i.e. 66.66%, indicating the toxicity of RB5 dye. Moreover, the area of each leave was also increased on using treated effluent with higher intensity of green color indicating the presence of more chloroplasts. It has already been reported that untreated effluents contain nutrients for plants but phytotoxicity dominate due to incomplete biodegradation of textile effluent in soil producing ethylene (Iqbal *et al.*, 2017).

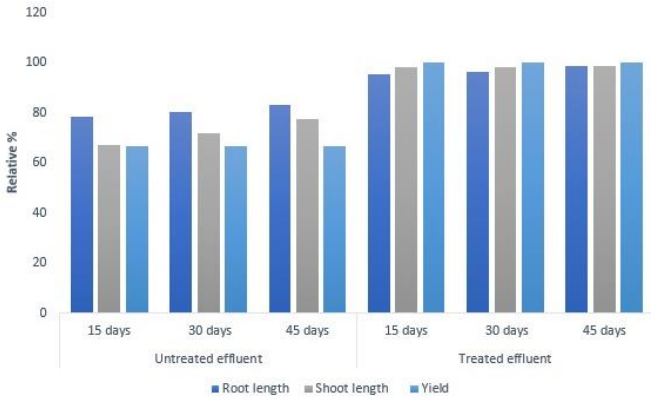

Figure 9. Effect of untreated and treated textile effluents on shoot length, root length and yield in relative percent.

The results obtained in case of spinach grown in pots concur with the researches previously reported about other plants. The ratio test for the assessment of phytotoxicity of various chemicals was also employed by other research groups (Kong *et al.*, 2007). For number of field plants the root and shoot elongation have been investigated to be inhibited containing various concentrations of synthetic effluent. The varied inhibitory concentrations for *T. aestivum* and *V. radiat, V. aconitifolia, V. sinensis, C. arietinum* were 30000 ppm, 20000 ppm, 15000 ppm, and 9000 ppm, respectively (Umesh *et al.*, 2016). Phytotoxic effect of dyes, causing reduction in length of root and shoot also been reported (Kosinkiewicz *et al.*, 1984). These studies have suggested that although, low concentration of dye had lesser toxic effects on seeds germination as compared to its higher amount in effluents. Contrarily, the low concentration of dye was examined to adversely affect relative percent of shoot elongation. Moreover, the significant toxic effect on root growth has been recorded with the high concentrations of the effluent. Similar

results were reported using several textile dyes (Moawad *et al.*, 2003). The previous results confirmed that synthetic textile effluent have toxic effect on all field and pot plants investigated. The present study also describes that pot plants are affected by azo dye even at lower concentration of 150 ppm. The toxic effect of dyes reported in these studies also suggested that the remediation of textile dyes present in the industry effluents bears crucial importance prior to their discharge into the environment.

DISCUSSION

The textile effluent was treated by undoped and Fe^{3+}doped ZnO discs, while the doped photocatalyst displayed much higher PCA as compared to undoped ZnO. This enhancement in PCA can be attributed to higher number of active sites available on greater area of exposed polar crystal surface of Fe^{3+}doped ZnO discs. The other important factors in this context are presence of surface defects such as oxygen vacancies (Xu *et al.*, 2013). The enhanced PCA of Fe^{3+}doped ZnO caused increase in degradation % of RB5 from 80.82% to 98.32% due to remarkable harvesting capability of solar radiation. The same test was employed by many other researchers (Kong et al., 2007) to assess the phytotoxicity of different chemicals.

Phytohormones like ethylene controls growth and yield of plants (Masood *et al.*, 2012). In the presence of ethylene, the stem has been reported to elongate to a minimum extent and also caused inhibition of growth of roots. The major cause of inhibition of overall growth is retardation of the mitotic process in the meristems of root and shoot (Nazar *et al.*, 2014). Within a few hours after ethylene is released, the number of mitotic figures declined in the stem apex. Similarly, it inhibits mitosis in the root apex upto 60%. Other researchers have also described the effect of textile effluents on plants like sorghum in terms of growth assessment along with biomass of plant were investigated. The results based on different concentration of textile water on plant height of sorghum indicated that control exhibited greater plant height, since there was no stress of effluents (Hayyat *et al.*, 2013).

***Conclusion*:** The nano scaled ZnO has been synthesized in undoped and doped forms as a heterogeneous photocatalyst to treat textile effluent. The optimized level of doping was determined on the basis of sunlight harvesting capability and bandgap energy. The highest % photocatalytic degradation of RB5 as a probe dye was carried out by Fe^{3+}-5-ZnO. The untreated and treated textile effluents were used to irrigate spinach plants and effect on the vegetative growth of the plants were examined. It has been concluded that textile effluents can be reused for irrigation after photocatalytic treatment to overcome the scarcity of water and toxic effects on the vegetation. The contaminant free crop can be grown and greater yield can be obtained by this irrigation practice.

***Acknowledgement*:** Authors are grateful to Endowment fund secretariat, university of Agriculture, Faisalabad for providing financial grant for this study.

REFERENCES

Adeleye, A.S., J.R. Conway, K. Garner, Y. Huang, Y. Su and A.A. Keller. 2016. Engineered nanomaterials for water treatment and remediation: costs, benefits, and applicability. Chem. Eng. J. 286:640-662.

Amin, M., A. Alazba and M. Shafiq. 2015. Adsorptive removal of reactive Black 5 from wastewater using bentonite clay: isotherms, kinetics and thermodynamics. Sustainability 7:15302.

Ashar, A., M. Iqbal, I.A. Bhatti, M.Z. Ahmad, K. Qureshi, J. Nisar and I.H. Bukhari. 2016. Synthesis, characterization and photocatalytic activity of ZnO flower and pseudo-sphere: Nonylphenol ethoxylate degradation under UV and solar irradiation. JAllC 678:126-136.

Ensink, J.H., T. Mahmood, W. Van der Hoek, L. Raschid-Sally and F.P. Amerasinghe. 2004. A nationwide assessment of wastewater use in Pakistan: An obscure activity or a vitally important one? Water Policy 6:197-206.

Faryal, R., F. Tahir and A. Hameed. 2007. Effect of wastewater irrigation on soil along with its micro and macro flora. Pak. J. Bot. 39:193-204.

Gahlout, M., S. Gupte and A. Gupte. 2013. Optimization of culture condition for enhanced decolorization and degradation of azo dye reactive violet 1 with concomitant production of ligninolytic enzymes by *Ganoderma cupreum* AG-1. 3 Biotech. 3:143-152.

Hayyat, M.U., R. Mahmood, S. Hassan and S. Rizwan. 2013. Effects of textile effluent on growth performance of *Sorghum vulgare* Pers CV. SSG-5000. Biologia 59:15-22.

Imran, M., B. Shaharoona, D.E. Crowley, A. Khalid, S. Hussain and M. Arshad. 2015. The stability of textile azo dyes in soil and their impact on microbial phospholipid fatty acid profiles. Ecotox. Environ. Safe. 120:163-168.

Iqbal, N., N.A. Khan, A. Ferrante, A. Trivellini, A. Francini and M. Khan. 2017. Ethylene role in plant growth, development and senescence: interaction with other phytohormones. Front. Plant Sci. 8:475-485.

Jadhav Umesh, D.R., D. Vishal, C. Ashok and P. Manohar. 2016. Phytotoxic effect of synthetic textile dye effluent on growth of five plant species. Trends Biotechnol. Res. 5:1-6.

Karmakar, D., S. Mandal, R. Kadam, P. Paulose, A. Rajarajan, T.K. Nath, A.K. Das, I. Dasgupta and G. Das. 2007. Ferromagnetism in Fe-doped ZnO nanocrystals: experiment and theory. PhRvB.75:DOI: 10.1103/PhysRevB.75.144404.

Kołodziejczak-Radzimska, A. and T. Jesionowski. 2014. Zinc oxide—from synthesis to application: a review. Materials 7:2833-2881.

Kong, W., Y. Zhu, Y. Liang, J. Zhang, F. Smith and M. Yang. 2007. Uptake of oxytetracycline and its phytotoxicity to alfalfa (*Medicago sativa* L.). Environ. Pollut. 147:187-193.

Kosinkiewicz, B., T. Wegrzyn and S. Pietr. 1984. Interaction between bacterial metabolites and some pesticides. II. Change of phytotoxicity of the herbicide Roneet by the phenolic metabolites of Arthrobacter sp. Acta Microbiol. Pol. 33:111-117.

Lavand, A.B. and Y.S. Malghe. 2016. Synthesis, characterization and visible light photocatalytic activity of carbon and iron modified ZnO. J. K. S. Uni. Sci. 30:65-74-85.

Li, Y., J.-Q. Shi, R.-J. Qu, M.-B. Feng, F. Liu, M. Wang and Z.-Y. Wang. 2012. Toxicity assessment on three direct dyes (D-BLL, D-GLN, D-3RNL) using oxidative stress bioassay and quantum parameter calculation. Ecotox. Environ. Safe. 86:132-140.

Mahmood, F., M. Shahid, S. Hussain, T. Shahzad, M. Tahir, M. Ijaz, A. Hussain, K. Mahmood, M. Imran and S.A.K. Babar. 2017. Potential plant growth-promoting strain Bacillus sp. SR-2-1/1 decolorized azo dyes through NADH-ubiquinone: oxidoreductase activity. Biores. Tech. 235:176-184.

Masood, A., N. Iqbal and N.A. Khan. 2012. Role of ethylene in alleviation of cadmium-induced photosynthetic capacity inhibition by sulphur in mustard. Plant Cell Environ. 35:524-533.

Moawad, H., W.M.A. El–Rahim and M. Khalafallah. 2003. Evaluation of biotoxicity of textile dyes using two bioassays. Journal of Basic Microbiology: Int. J. Biochem. Physiol. Genet. Morpho. Ecolo. Microorg. 43:218-229.

Nazar, R., M.I.R. Khan, N. Iqbal, A. Masood and N.A. Khan. 2014. Involvement of ethylene in reversal of salt-inhibited photosynthesis by sulfur in mustard. Physiol. Plant. 152:331-344.

Neoh, C.H., C.Y. Lam, C.K. Lim, A. Yahya, H.H. Bay, Z. Ibrahim and Z.Z. Noor. 2015. Biodecolorization of recalcitrant dye as the sole source of nutrition using *Curvularia clavata* NZ2 and decolorization ability of its crude enzymes. Environ. Sci. Pollut. Res. Int. 22:11669-11678.

O'Neill, C., F.R. Hawkes, D.L. Hawkes, N.D. Lourenço, H.M. Pinheiro and W. Delée. 1999. Colour in textile effluents–sources, measurement, discharge consents and simulation: a review. J. Chem. Technol. Biotechnol. 74:1009-1018.

Reemtsma, T. 2001. Prospects of toxicity-directed wastewater analysis. Anal. Chim. Acta 426:279-287.

Rekha, K., M. Nirmala, M.G. Nair and A. Anukaliani. 2010. Structural, optical, photocatalytic and antibacterial activity of zinc oxide and manganese doped zinc oxide nanoparticles. Physica B: Condensed Matter. 405:3180-3185.

Shafqat, M., A. Khalid, T. Mahmood, M.T. Siddique, J.I. Han and M.Y. Habteselassie. 2017. Evaluation of bacteria isolated from textile wastewater and rhizosphere to simultaneously degrade azo dyes and promote plant growth. J. Chem. Technol. Biotechnol. 92:2760-2768.

Sun, Y., L. Chen, Y. Bao, Y. Zhang, J. Wang, M. Fu, J. Wu and D. Ye. 2016. The applications of morphology controlled ZnO in catalysis. Catalysts 6:188-200.

Vafaei, F., A. Khataee, A. Movafeghi, S.S. Lisar and M. Zarei. 2012. Bioremoval of an azo dye by Azolla filiculoides: Study of growth, photosynthetic pigments and antioxidant enzymes status. Int. Biodeterior. Biodegrad. 75:194-200.

Weisburger, J.H. 2002. Comments on the history and importance of aromatic and heterocyclic amines in public health. Mutat. Res-Fund. Mol. M. 506:9-20.

Wu, X., Z. Wei, L. Zhang, X. Wang, H. Yang and J. Jiang. 2014. Optical and magnetic properties of Fe doped ZnO nanoparticles obtained by hydrothermal synthesis. J. Nanomater.4: DOI:10.1186/1556-276X-8-536.

Xu, L., B. Wei, W. Liu, H. Zhang, C. Su and J. Che. 2013. Flower-like ZnO-Ag 2 O composites: precipitation synthesis and photocatalytic activity. Nanoscale. Res. Lett. 8:536. 8: DOI:10.1186/1556-276X-8-536.

Zhang, W., W. Liu, J. Zhang, H. Zhao, Y. Zhang, X. Quan and Y. Jin. 2012. Characterisation of acute toxicity, genotoxicity and oxidative stress posed by textile effluent on zebrafish. J. Environ. Sci. 24:019-2027.